

# Anisotropic Tissue Motion Induced by Acupuncture Needling Along Intermuscular Connective Tissue Planes

James R. Fox, BS, MS,<sup>1</sup> Weili Gray, MD,<sup>1,2</sup> Cathryn Koptiuch, BS,<sup>1</sup>  
Gary J. Badger, MS,<sup>3</sup> and Helene M. Langevin, MD<sup>1,4</sup>

## Abstract

**Objectives:** Acupuncture needle manipulation causes mechanical deformation of connective tissue, which in turn results in mechanical stimulation of fibroblasts, with active changes in cell shape and autocrine purinergic signaling. We have previously shown using ultrasound elastography in humans that acupuncture needle manipulation causes measurable movement of tissue up to several centimeters away from the needle. The goal of this study was to quantify the spatial pattern of tissue displacement and deformation (shear strain) in response to acupuncture needling along an intermuscular connective tissue plane compared with needling over the belly of a muscle.

**Design:** Eleven (11) healthy human subjects underwent a single testing session during which robotic acupuncture needling was performed while recording tissue displacement using ultrasound. Outcome measures were axial and lateral tissue displacement as well as lateral shear strain calculated using ultrasound elastography postprocessing.

**Results:** Tissue displacement and strain extended further in the longitudinal direction when needling between muscles, and in the transverse direction when needling over the belly of a muscle.

**Conclusions:** The anisotropic tissue motion observed in this study may influence the spatial distribution of local connective tissue cellular responses following acupuncture needle manipulation.

## Introduction

**D**URING MANUAL ACUPUNCTURE treatments, acupuncture needles are traditionally manipulated using a combination of rotation and pistoning (up-and-down) motion. Studies in animals have shown that, in response to this mechanical stimulation, local connective tissue fibroblasts undergo active cytoskeletal remodeling and expansion up to several centimeters away from the needle.<sup>1</sup> Mounting evidence suggests that this mechanically induced response of fibroblasts is accompanied by analgesic effects induced by autocrine/paracrine purinergic signaling.<sup>2,3</sup> Thus, the needle grasp phenomenon is a measurable phenomenon with potential ties to both connective tissue remodeling and peripheral sensory modulation.

An important remaining question is: how far from the needle do these connective tissue responses occur in humans? Because they are caused by the needle interacting with the collagen network, it is plausible that these cellular responses could be influenced by local differences in the orientation of collagen fiber within connective tissue. For example, we

know that, in the thigh, collagen fibers located over the belly of muscles are organized in oblique, criss-crossing layers.<sup>4</sup> In contrast, collagen fibers along intermuscular connective tissue planes are predominantly longitudinal as they follow the course of neurovascular bundles. Thus, mechanical signals generated by an acupuncture needle could be propagated further, or more efficiently, in the longitudinal direction when needled along intermuscular “channels” of collagenous connective tissue.

It was previously shown that robotically controlled oscillation of an inserted acupuncture needle caused displacement of tissue that was measurable using ultrasound elastography in normal human subjects.<sup>5,6</sup> The goal of this study was to use these techniques to measure the tissue displacement and strain patterns resulting from acupuncture needling along a connective tissue plane separating two muscles as well as a control location over the belly of a muscle. It was hypothesized that tissue displacement and strain are greater in the longitudinal direction compared with the transverse direction when needling along the connective tissue plane, but not at the control location.

Departments of <sup>1</sup>Neurological Sciences, <sup>2</sup>Anesthesiology, and <sup>3</sup>Medical Biostatistics, University of Vermont College of Medicine, Burlington, VT.

<sup>4</sup>Division of Preventive Medicine, Brigham and Women’s Hospital, Harvard Medical School, Boston, MA.

The contents of this article are solely the responsibility of the authors and do not necessarily represent the official views of the National Center for Complementary and Alternative Medicine, National Institutes of Health.

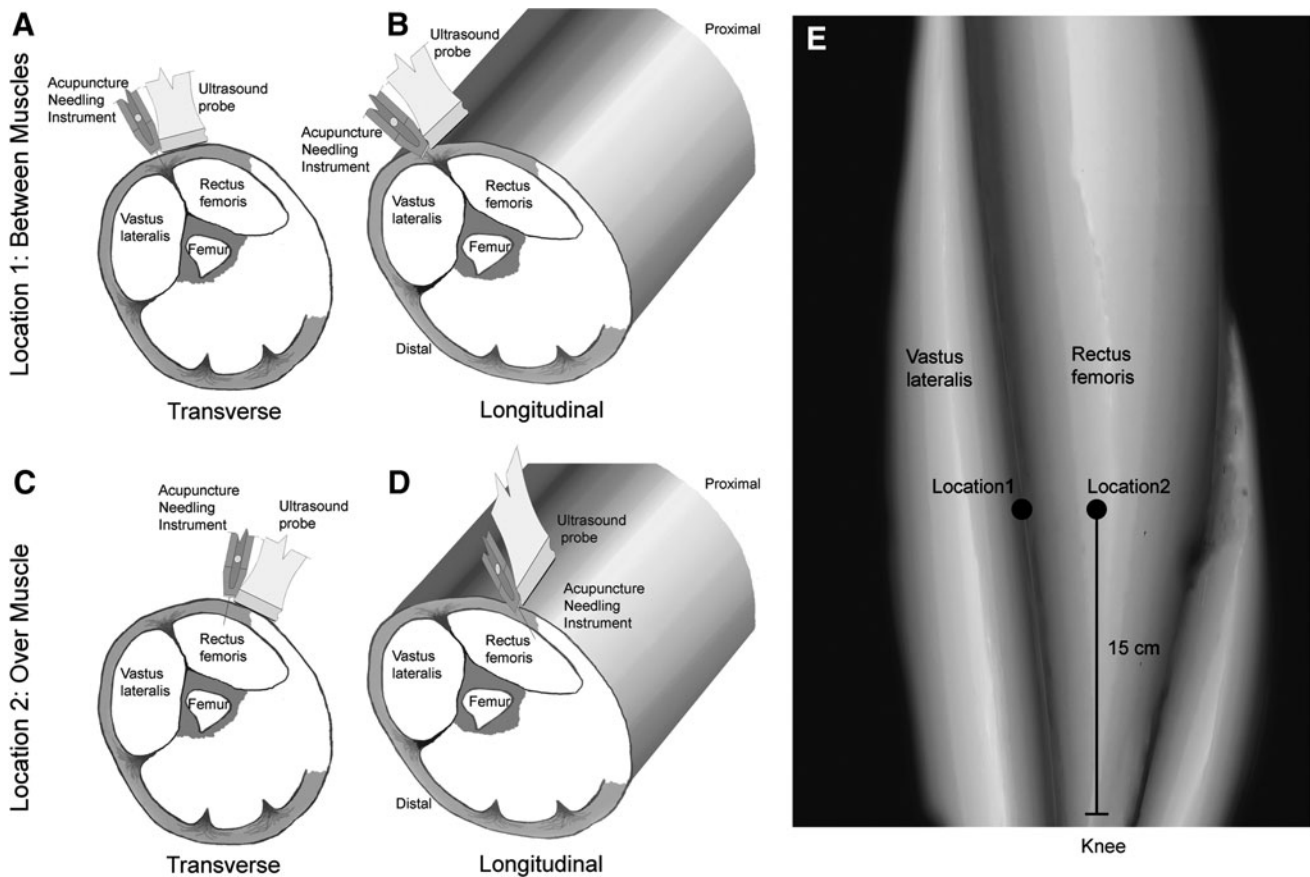


**FIG. 1.** Schematic representation of the needling locations and orientations on the anterior thigh tested in this study. Locations 1 (between muscles) and 2 (over muscle) are shown in a surface representation of the thigh (**E**) as well as cross-sections (**A–D**). Transverse (**A, C**) and longitudinal (**B, D**) orientations of the ultrasound probe are illustrated in the cross-sections for both locations.

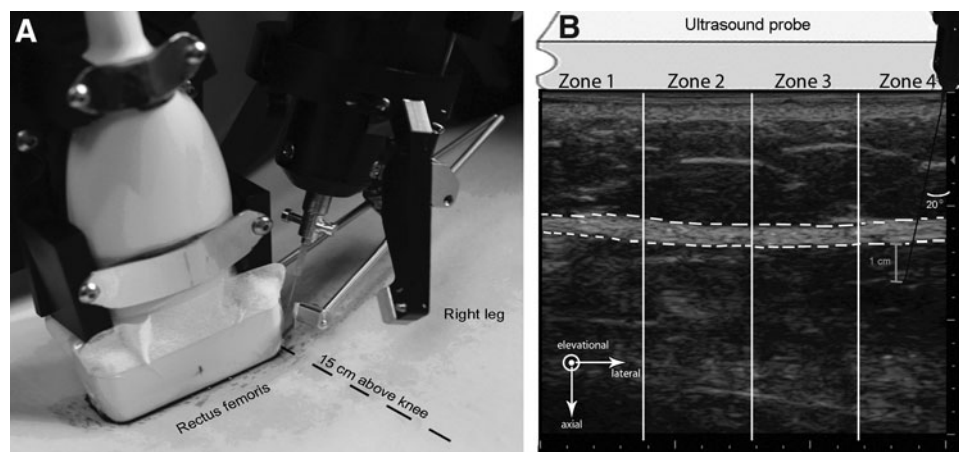
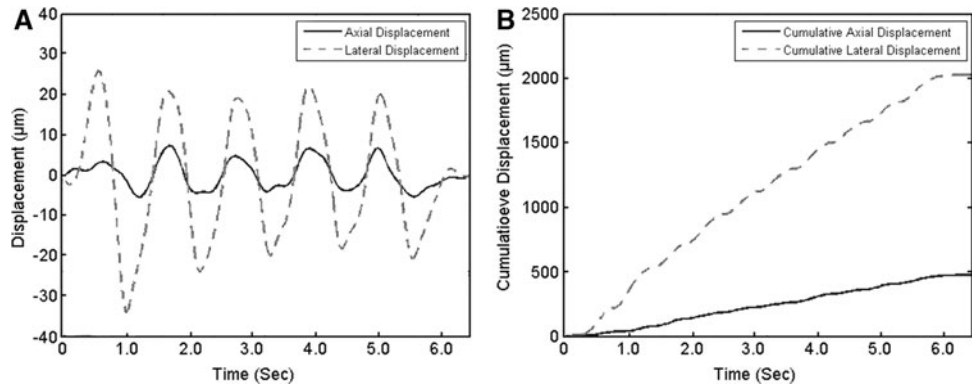


**FIG. 2.** Robotic needling instrument and location of needling in relation to ultrasound transducer (**A**) and example of ultrasound image with relationship of ultrasound probe and acupuncture needling instrument (**B**). The location of the acupuncture needle is shown on the right-hand corner of the ultrasound image. The region of interest encompassing the perimuscular connective tissue is delineated by the dashed white lines. The 4 zones used for the detailed analysis of tissue displacement and strain are also indicated, with Zone 1 being furthest away from the needle and Zone 4 including the needle. Arrows indicate the directions of lateral (parallel to the skin) and axial (parallel to the needle) tissue displacement in the ultrasound image plane evaluated in this study. Elevational displacement (not measured in this study) represents displacement in and out of the ultrasound image plane. X- and Y-axis major unit divisions represent 1 cm.

**FIG. 3.** Examples of plots for axial and lateral tissue displacement for each ultrasound frame (A) and cumulative axial and lateral tissue displacement (B).



**Materials and Methods**

Eleven (11) human subjects (6 male and 5 female, ages 21–57) were tested. The study was approved by the University of Vermont Institutional Review Board (CHRMS 07-025) and in compliance with the Helsinki Declaration. All subjects provided informed consent. Subjects were recruited by advertisements at the University of Vermont and associated facilities. One (1) subject (female) did not complete the study due to pain during needling. Each subject was tested once at 2 locations on the anterior thigh bilaterally (4 points total) (Fig. 1A).

*Location 1*

The area to be needled was between muscles (Fig. 1A and B). The needle was inserted at the lateral edge of the rectus femoris, 15 cm rostral to the patella, between rectus femoris and vastus lateralis muscles.

*Location 2*

The area to be needled was over muscle (Fig. 1C and D). The needle was inserted over the belly of the rectus femoris, 2 cm medial to location 1.

At each location, the right and left sides of the body were randomized to transverse (Fig. 1A and C) versus longitudinal (Fig. 1B and D) needling orientations.

In both orientations, the acupuncture needle insertion and oscillation were performed by a computer-controlled acupuncture needling instrument (Fig. 2A). The angle of needle insertion was 20° to the vertical, and the needle was inserted in the plane of the ultrasound image, either transversely or longitudinally such that the needle was in the upper right portion of the image (Fig. 2B).

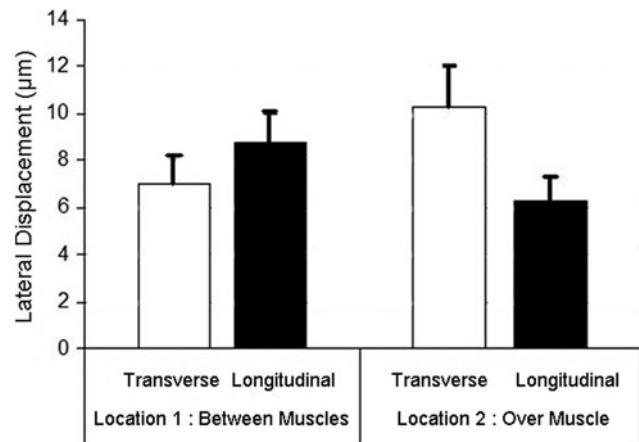
For each test, the needle was inserted 1 cm beyond the perimuscular fascia as determined by ultrasound (Fig. 2B). Once inserted, the needle underwent five cycles of oscillation of 5 mm amplitude and 1-Hz frequency. The raw, ultrasound radio frequency (RF) data were acquired at 25 frames/sec using a Terason 3000 scanner (linear array transducer 10–12 MHz) and were used for postprocessing analysis.

Tissue axial and lateral displacements were estimated using elastography cross-correlation techniques.<sup>7,8</sup> The term “displacement” refers to the axial or lateral motion of the tissue between 2 successively acquired ultrasound frames (i.e., after 40 ms have elapsed). Axial displacement refers to tissue displacement along the ultrasound beam (perpendicular to the skin), while lateral displacement refers to tissue displacement perpendicular to the ultrasound beam (parallel









to the skin) (see axes represented in Fig. 2B). All tissue displacement and strain calculations were performed within a region of interest (ROI) centered on and encompassing the entire thickness of the perimuscular connective tissue and the whole width of the image (see outlined area in Fig. 2B).

Average tissue displacement per ultrasound frame was calculated over the whole width of the image, as well as in 4 zones of equal width as shown in Figure 2B. Numbered from left to right, zone 1 was furthest away from the needle and zone 4 included the needle. Cumulative axial and lateral tissue displacement also was calculated over the 5 oscillations and was reported as the average per 1 full oscillation (upward and downward motion of the needle). The relationship between tissue displacement per ultrasound frame and cumulative tissue displacement is illustrated in Figure 3. Shear strain was calculated between the layers superficial and deep to the echolucent band separating the echogenic band closest to muscle (perimuscular fascia) and the echogenic band immediately superficial to it as previously described.<sup>9</sup>

For each outcome measure, repeated-measures analysis of variance (SAS, PROC MIXED) was used to evaluate the significance of main effects of location (between versus over muscle) and orientation (transverse versus longitudinal) and their interaction. In order to satisfy the Gaussian



**FIG. 4.** Lateral tissue displacement (between 2 successive ultrasound frames) over the whole width of the image at the 2 needling locations and 2 orientations (transverse and longitudinal). There was a significant statistical interaction between location and orientation ( $p < 0.01$ ), with greater longitudinal displacement at Location 1 and greater transverse displacement at Location 2. Error bars represent standard errors.

	Zone 1	Zone 2	Zone 3	Zone 4
Location 1: Between Muscles	4.7±0.7  6.7±1.0	5.2±0.7  6.7±0.9	8.0±1.3  7.1±1.2	19.1±3.8  9.2±1.8
Location 2: Over Muscle	3.6±0.6  8.1±1.3	4.2±0.6  9.3±1.3	6.0±1.0  10.5±1.8	13.2±2.6  15.3±3.0
Tissue Displacement p value (interaction)	p=.077	p=.016	p=.023	p=.012

**FIG. 5.** Schematic representation of longitudinal and transverse displacement at both needling locations over 1 needling oscillation cycle. Tissue displacement ( $\mu\text{m}$ ) is plotted in 4 zones, with Zone 1 being furthest away from the needle and Zone 4 including the needle (see Fig. 2 for zone locations). Values represent mean  $\pm$  standard error of the mean.

distributional assumption, data were log transformed prior to analysis. All means presented represent geometric means with corresponding standard errors computed using the Delta method. Analyses were performed using SAS statistical software (SAS Institute, Cary, NC). Statistical significance was determined using  $\alpha=0.05$ .

**Results**

First the average lateral displacement between 2 successive ultrasound frames within perimuscular connective tissue over the whole width of the image was examined. Tissue displacement was significantly different in the longitudinal needling orientation compared with the transverse needling orientation, and this difference was dependent on the needling location (between muscles versus over muscle) ( $F_{1,24}=8.0$ ,

$p < 0.01$  for interaction, Fig. 4). When the needle was inserted between 2 muscles (Location 1), average tissue displacement between 2 consecutive frames was greater in the longitudinal than the transverse location orientation. In contrast, when the needle was inserted over the muscle belly (Location 2), displacement was greater in the transverse than the longitudinal orientation.

In order to further examine possible differences in tissue behavior between needle locations as a function of distance away from the needle, lateral tissue displacement was calculated in 4 zones, where Zone 1 is furthest away from the needle and Zone 4 includes the needle. Figure 5 illustrates the relative magnitude of tissue displacement in the longitudinal and transverse orientations in the 4 zones, and shows that the preponderance of longitudinal displacement when the needle is inserted between muscles occurs nearest the

TABLE 1. AXIAL AND LATERAL TISSUE DISPLACEMENT AND LATERAL SHEAR STRAIN

Ultrasound image zones	Location 1: between muscles		Location 2: over muscle		Location p-value	Orientation p-value	Interaction p-value
	Transverse	Longitudinal	Transverse	Longitudinal			
<b>Zone 1</b>							
Axial displacement	86.3 $\pm$ 25.8	156.9 $\pm$ 46.9	151.2 $\pm$ 45.2	131.9 $\pm$ 39.4	0.325	0.241	0.068
Lateral displacement	183.5 $\pm$ 26.7	126.5 $\pm$ 18.4	233.1 $\pm$ 33.9	100.6 $\pm$ 14.6	0.965	<0.0001	0.057
Shear strain	3.2 $\pm$ 0.6	3.3 $\pm$ 0.6	3.2 $\pm$ 0.6	2.2 $\pm$ 0.4	0.189	0.294	0.198
<b>Zone 2</b>							
Axial displacement	45.6 $\pm$ 13.8	142.3 $\pm$ 43.2	110.4 $\pm$ 33.5	94.3 $\pm$ 28.6	0.114	0.002	0.0002
Lateral displacement	182.5 $\pm$ 24.0	140.2 $\pm$ 18.4	270.3 $\pm$ 35.5	119.6 $\pm$ 15.7	0.244	<0.0001	0.009
Shear strain	2.7 $\pm$ 0.5	3.9 $\pm$ 0.8	3.6 $\pm$ 0.7	2.3 $\pm$ 0.5	0.539	0.85	0.038
<b>Zone 3</b>							
Axial displacement	68.8 $\pm$ 23.7	213.8 $\pm$ 74.8	130.2 $\pm$ 44.9	131.1 $\pm$ 45.3	0.669	0.003	0.003
Lateral displacement	195.9 $\pm$ 30.7	214.4 $\pm$ 33.6	303.2 $\pm$ 47.4	170.1 $\pm$ 26.6	0.041	0.059	0.012
Shear strain	3.3 $\pm$ 0.6	5.4 $\pm$ 0.9	4.4 $\pm$ 0.7	4.2 $\pm$ 0.7	0.809	0.209	0.125
<b>Zone 4</b>							
Axial displacement	244.7 $\pm$ 74.6	1051.5 $\pm$ 320.3	361.1 $\pm$ 110.0	526.4 $\pm$ 160.4	0.489	0.0003	0.019
Lateral displacement	251.7 $\pm$ 48.4	515.4 $\pm$ 99.2	441.4 $\pm$ 84.9	372.8 $\pm$ 71.7	0.456	0.094	0.009

Axial and lateral tissue displacement values represent cumulative displacement ( $\mu\text{m}$ ) over 1 complete needle oscillation (up and down). Shear strain (%) represents the percent shear deformation between layers within perimuscular connective tissue. Displacement and strain values are expressed as mean  $\pm$  standard error. The p-values represent differences between location (between muscles vs. over muscles), orientation (transverse vs. longitudinal), and the interaction of the 2 conditions. Note: lateral shear strain was not calculated for Zone 4 due to the relatively large axial motion in the zone closest to the needle.

needle (Zone 4). Tissue displacement became greater in the longitudinal direction as one got closer to the intermuscular connective tissue plane, and became greater in the transverse direction as one moved away from the connective tissue plane and over the muscle belly.

Additional measurement of cumulative tissue displacement (axial and lateral) and shear strain within the perimuscular fascia are summarized in Table 1. Significant statistical interactions between needling location and needling orientation were present for the majority of these measurements in zones 2, 3, and 4. The magnitude of longitudinal tissue displacement and strain was always greater when the needle was inserted between 2 muscles, compared with insertion over the muscle itself.

## Discussion

In response to acupuncture needling, tissue displacement was anisotropic, with longitudinal motion predominant when the needle was inserted between muscles, and transverse motion when the needle was inserted into the muscle. This suggests that the spatial distribution of cellular responses to acupuncture needling may be different when needling along intermuscular connective tissue versus needling over the belly of a muscle. A previous study by Julias et al. addressed a related question using an *in vitro* fibroblast-populated collagen gel model in which an acupuncture needle was inserted and rotated to examine collagen and fibroblast alignment immediately following needle rotation.<sup>10</sup> Elliptical gels mimicking intermuscular connective tissue planes constrained on 2 sides by muscle were compared with circular gels without such anisotropic boundary restrictions. Collagen and cell alignment was isotropic in the circular gels, but anisotropic in the elliptical gels with increased alignment in the transverse axis of the gel, presumably indicating increased stress in that direction. This study's results are consistent with Julias' study because the current study measured displacement and strain (percent change in length) as opposed to stress (force divided by cross sectional area). Greater tissue movement and strain in the longitudinal direction in this study is consistent with smaller stress due to less restricted boundary conditions, compared with the transverse direction.

An important related question is whether fibroblasts within areolar connective tissue respond to local stress or local strain. The answer to this question may depend on the type of response that one is measuring in response to acupuncture needling. Julias measured cell alignment immediately after needle rotation, which may be stress dependent. In contrast, slower, Rho-dependent cytoskeletal remodeling, which takes ~30 minutes, may be a response to local tissue deformation (strain) as opposed to local tissue stress.<sup>11,12</sup> Further studies in animal models will be needed to answer this question.

## Conclusions

This study demonstrates that the needling of intermuscular connective tissue results in an enhanced longitudinal displacement and strain pattern during acupuncture needling, compared with needling over a muscle where the displacement/strain pattern is predominantly transverse. This difference may affect the spatial distribution of cellular responses to acupuncture needling within local connective tissue.

## Acknowledgments

The authors thank Nicole Bouffard for creating the illustrations. This project was supported by Research Grants RO1 AT003479 from the National Center for Complementary and Alternative Medicine. Testing of human subjects was conducted at the University of Vermont General Clinical Research Center at Fletcher Allen Health Care supported by NIH Center for Research Resources Grant MO1 RR00109.

## Author Disclosure Statement

No competing financial interests exist.

## References

1. Langevin HM, Bouffard NA, Badger GJ, et al. Subcutaneous tissue fibroblast cytoskeletal remodeling induced by acupuncture: Evidence for a mechanotransduction-based mechanism. *J Cell Physiol* 2006;207:767–774.
2. Goldman N, Chen M, Fujita T, et al. Adenosine A1 receptors mediate local anti-nociceptive effects of acupuncture. *Nat Neurosci* 2010;13:883–888.
3. Langevin. CREGE, In Press.
4. Benetazzo L, Bizzego A, De Caro R, et al. 3D reconstruction of the crural and thoracolumbar fasciae. *Surg Radiol Anat* 2011;33:855–862.
5. Langevin HM, Konofagou EE, Badger GJ, et al. Tissue displacements during acupuncture using ultrasound elastography techniques. *Ultrasound Med Biol* 2004;30:1173–1183.
6. Langevin HM, Rizzo DM, Fox JR, et al. Dynamic morphometric characterization of local connective tissue network structure in humans using ultrasound. *BMC Systems Biol* 2007;1:25.
7. Ophir J, Cespedes I, Ponnekanti H, et al. Elastography: A quantitative method for imaging the elasticity of biological tissues. *Ultrason Imaging* 1991;1:111–134.
8. Konofagou E, Ophir J. A new elastographic method for estimation and imaging of lateral displacements, lateral strains, corrected axial strains and Poisson's ratios in tissues. *Ultrasound Med Biol* 1998;24:1183–1199.
9. Langevin HM, Fox JR, Koptiuch C, et al. Reduced thoracolumbar fascia shear strain in human chronic low back pain. *BMC Musculoskel Disord* 2011;12:203.
10. Julias M, Edgar LT, Buettner HM, Shreiber DI. An in vitro assay of collagen fiber alignment by acupuncture needle rotation. *Biomed Eng Online* 2008;7:19.
11. Langevin HM, Bouffard NA, Badger GJ, et al. Dynamic fibroblast cytoskeletal response to subcutaneous tissue stretch ex vivo and in vivo. *Am J Physiol Cell Physiol* 2005;288:C747–756.
12. Langevin HM, Storch KN, Cipolla MJ, et al. Fibroblast spreading induced by connective tissue stretch involves intracellular redistribution of alpha- and beta-actin. *Histochem Cell Biol* 2006;125:487–495.

Address correspondence to:  
 Helene M. Langevin, MD  
 Department of Neurological Sciences  
 University of Vermont College of Medicine  
 Burlington, VT 05405

E-mail: hlangevin@partners.org